

CERN LIBRARIES, GENEVA



CM-P00055809

CERN/EEC-74/1

2/1/74

LETTER OF INTENTION TO THE EEC

LARGE ANGLE AND HIGH  $P_T$  TRIGGER USING THE  $\Omega$  FACILITY

R. HARTUNG, B. HENIN, K. RUNGE, O. SCHAILE, C. WEBER,  
Freiburg

F. BRUN, M. CRIBIER, J.R. HUBBARD, L. MOSCOSO,  
A. MULLER, S. ZYLBERAJCH,  
Saclay

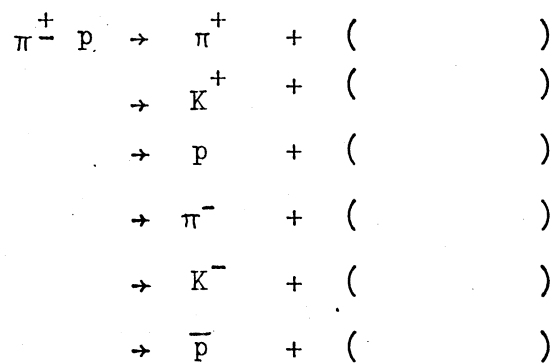
LETTER OF INTENTION

Large Angle and High  $P_T$  Trigger Using the  $\Omega$  Facility

We propose to use the  $\Omega$  facility with incident  $\pi$ 's between 8 and 16 GeV/c for the following projects :

- 1) To study two-body and quasi-two-body reactions with large momentum transfer ( $1 < -t < 5 \text{ (GeV/c)}^2$ ) ;
- 2) To trigger on particles with large  $P_T$  and  $x > 0$ , detecting all associated charged particles.

The following reactions can be studied :



The physical interest of the proposal is straightforward . The cross sections involved are of the order of tens of nanobarns. Two-body and quasi-two-body data are limited to momentum transfer below  $1 \text{ (GeV/c)}^2$  in most bubble chamber experiments due to the small cross sections. Conventional counter experiments are generally limited by the acceptance of the magnets and by the complexity of the topologies .( The exception is elastic scattering, where several successful experiments have been performed. Ref. [1,2] ).

The differential elastic cross sections in Fig. 1 exhibit significant structure at large c.m. scattering angles. Large-angle structure can also be expected for most inelastic reactions.

The physics at large  $P_T$  is also important, even at PS energies. We will be able to detect particles with at least one high  $P_T$  charged particle, and to measure inclusive and exclusive reactions (although neutral particles will not be detected). The cross sections for these reactions are very small and inaccessible to bubble chambers.

In this letter we attempt to show that this kind of physics can be done very soon with the existing  $\Omega$  facility.

Experimental set-up :

The basic idea of the experiment is to trigger on an

energetic, wide-angle, forward-going charged particle (large  $P_T$  or high  $t$ ). Omega's central spark chambers detect the associated charged particles.

Figure 2 shows the proposed set-up. This is the standard  $\Omega$  disposition, except that the hodoscopes in front of and behind the low-pressure Čerenkov counter are in central positions. The high-pressure Čerenkov is only necessary if we want to identify K's.

#### Trigger and Acceptance :

In order to avoid saturating the trigger rate, we must eliminate all events with low  $P_T$ , because the corresponding cross sections are large. The deflecting power of the  $\Omega$  magnet is used to select particles with large  $P_T$ .

Figures 3(a,c) show the impact of charged particles on a vertical plane 6 meters behind the target. Only high  $P_T$  particles cross this plane on the side opposite to the non-interacting beam tracks.

In Fig. 4 we show the impact of particles with different momentum transfer ( $t$ ), for incident  $\pi$ 's of 8 GeV/c and for two-body or quasi-two-body reactions. It can be seen that the  $\Omega$  magnetic field defocuses particles on one side and focuses high- $t$  particles on the other side. By symmetry we get a similar figure for particles with a charge opposite to the charge of the beam.

Figure 5 shows charged particles of both signs with different  $t$ . Placing the present hodoscope symmetrically as shown in the figure, we obtain the following acceptances, for incident  $\pi$ 's at 8 GeV/c (without the high-pressure Čerenkov) :

- 1) Acceptance for the  $t$ -distribution (Fig. 6) ;
- 2) Acceptance for the  $P_T$  vs.  $P_L$  plot. (Fig. 7).

These acceptances are valid for both positive and negative particles. At 16 GeV/c, particles with  $t = 0$  hit the edge counters, and we must reduce the effective width of the hodoscope.

At any energy we have considerable flexibility to reduce the acceptance for low  $P_T$ . The choices are as follows :

- 1) Switch off the edge hodoscope counters ;
- 2) Trigger on the correlation between  
Hodoscope 1 and Hodoscope 2.

We can eliminate the lowest  $P_T$  on both sides by choosing the appropriate front-back hodoscope correlation. Fig. 8 shows the front-back correlation for all particles coming from the target for interactions at 8 GeV/c. The zone  $P_T < 1$  GeV/c is shown with vertical hatching on the same figure. Eliminating  $P_T < 1$  GeV/c by the electronic logic, we obtain the acceptances shown in Fig. 6 and 9. For elastic scattering we detect both the forward and backward hemispheres and obtain the acceptance of Fig. 10. We also show the acceptance possible if we can tolerate smaller  $P_T$  for beam-unlike particles.

The Čerenkov counters are used for identify the particles. If the high-pressure Čerenkov is used for identifying K's it is not possible to detect particles with both signs.

Our trigger would be a H1-H2 correlation, with one or two Čerenkov signals or vetoes if needed. The gases in the Čerenkovs depend on the energy and on the reaction studied. The H1-H2 correlation has to be adjusted for each energy.

Trigger Rate :

For most of the reactions to be studied we can tolerate a parasite beam track crossing the optical spark chambers. This is because a high- $P_T$  beam-like particle which triggers the system is never confused with a beam track. Thus, we can accept more beam intensity than the standard  $\Omega$  experiments.

With a 60 cm target and beam intensity between 1 and  $5 \times 10^5$  per burst, we get from 1 to 5 events / n-barn/day. The trigger rate can be reduced as much as necessary by reducing the acceptance for low  $P_T$ . An inspection of bubble-chamber data indicates that we cannot accept  $P_T$  below 1 GeV/c if we do not want to saturate the trigger.

The background trigger rate has to be measured. We propose to do so during a test of our trigger.

Conclusion :

This letter shows that we could perform an extensive experimental physics program for large- $t$  and high -  $P_T$  reactions using the existing equipment . Obviously we can not study all the reactions at several energies in the limited time which is available .

We are requesting a test at the beginning of the  $\Omega$  run in Spring 1974 and, if successful, production time for one or several reactions at one or several energies at the end of 1974.

We would also like to point out that this kind of physics can be extended to the highest  $P_T$  and to  $90^\circ$  in the c.m., where the cross sections are of the order of 1 n-barn  $/(\text{GeV}/c)^2$ , if  $\Omega$  is equipped with a fast central detector. On the other hand, if the proposed experiment is successful it can be completed with incident  $K$ 's between 10 and 30 GeV/c with the R-F separated beam .

## REFERENCES

- [1] C. BAGLIN, Phys. Letters B47, 85 (1973)
- [2] C. BAGLIN, Phys. Letters B47, 89 (1973).



FIGURE CAPTIONS.

Fig. 1 - Differential cross sections, as given in ref. [1]  
for  $\pi^+p$  elastic scattering.

For  $2 < -t < 5$   $(\text{GeV}/c)^2$ , the cross sections at the  
higher energies range from 1000 to 10 nbarn  $/(\text{GeV}/c)^2$ .

Fig. 2 - Experimental set-up.

H1 and H2 are centrally located in the figure,  
but they can be moved slightly to one side in order  
to decrease the acceptance for beam-like particles  
with low  $P_T$ . The high-pressure Čerenkov decreases  
the acceptance, but it is not required for all the  
reactions proposed. It could also be placed on one  
side to identify particles of only one sign.

Fig. 3 - Impact of charged particles on a vertical plane  
6 meters behind the target.

a)  $P_T = 0.4 \text{ GeV}/c$

b)  $P_T = 1 \text{ GeV}/c$

c)  $P_T = 1.6 \text{ GeV}/c$

All low -  $P_T$  particles cross this plane on the same  
side of the  $\Omega$  axis

Fig. 4 - Impact of particles with different momentum transfer ( $t$ )  
for elastic or quasi-elastic reactions. The hatched  
area on the left contains all particles with  $P_T$  lower  
than 1  $\text{GeV}/c$ .

Fig. 5 - Impact of particles of both signs for different values of  $t$ . The rectangle in the middle represents the first hodoscope H1.

Fig. 6 - Acceptance as a function of  $t$  <sup>FOR TWO BODY REACTIONS</sup> for particles hitting hodoscope H1. The dotted line shows the acceptance reduced by the proposed H1. H2 correlation.

Fig. 7 - Peyrou plot acceptance for particles hitting H1 (centrally placed). The values of  $t$  are shown for elastic and quasi-elastic reactions (i.e., the edge of the Peyrou plot).

Fig. 8 - Correlation between the planes H1 and H2 containing the two hodoscopes. Positive tracks fill the lower zone of correlation ; negative tracks, the upper . The dashed rectangle denotes the dimensions of the two hodoscopes . The vertically-hatched regions correspond to  $P_{\perp} < 1 \text{ GeV}/c$  . The horizontally- hatched regions, with high  $P_{\perp}$ , correspond to the H1. H2 correlation used in our acceptance calculations.

Fig. 9 - The Peyrou plot acceptance for particles satisfying the proposed H1. H2 correlation.

Fig. 10 - Elastic acceptance obtained when the H1. H2 correlation is required for the forward-going pion

or proton. The dashed line shows the acceptance possible in  $\pi^-p$  elastic scattering when the correlation is required for the  $\pi^-$ , but all protons hitting H1 are accepted.

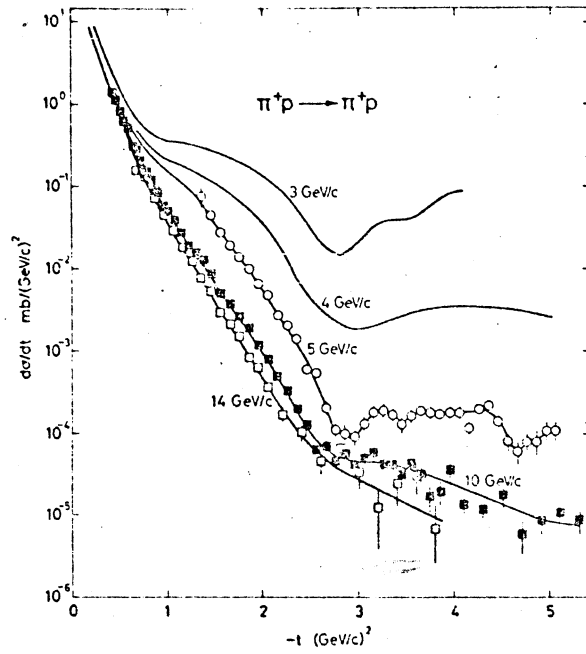


Fig. 3. The differential cross-section for  $\pi^+p$  elastic scattering as a function of  $-t$  in the region  $0 < -t < 5$   $(\text{GeV}/c)^2$ . The curves at 3 and 4  $\text{GeV}/c$  are taken from Brabson et al. [3], the data at 5, 10, and 14  $\text{GeV}/c$  are from Eide et al. [1], this experiment, and from Rubinstein et al. [8], respectively.

Fig. 1

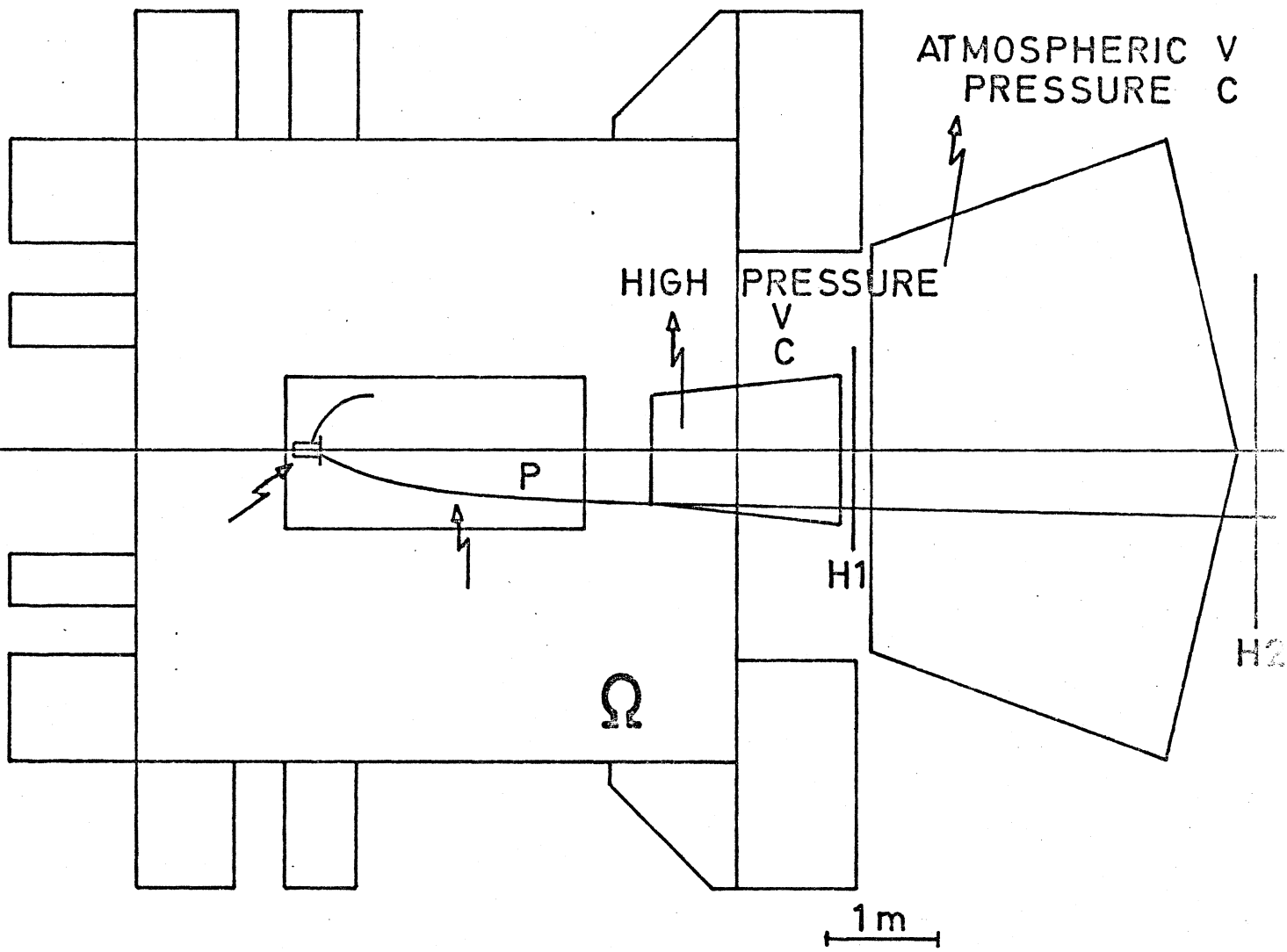


Fig. 2

8 GEV/c

$P_T = 0.4 \text{ GeV}$

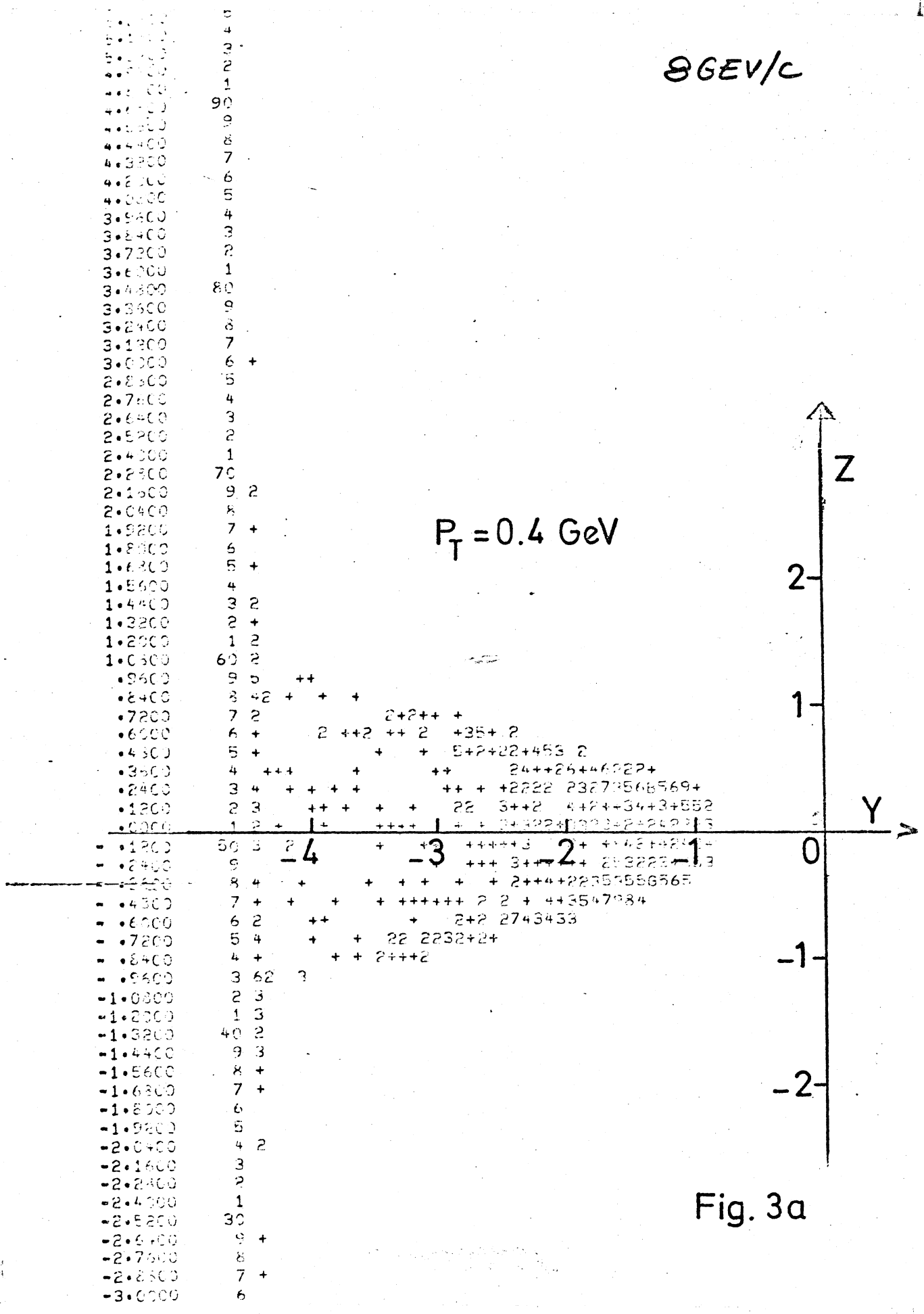


Fig. 3a

8 GEV/c

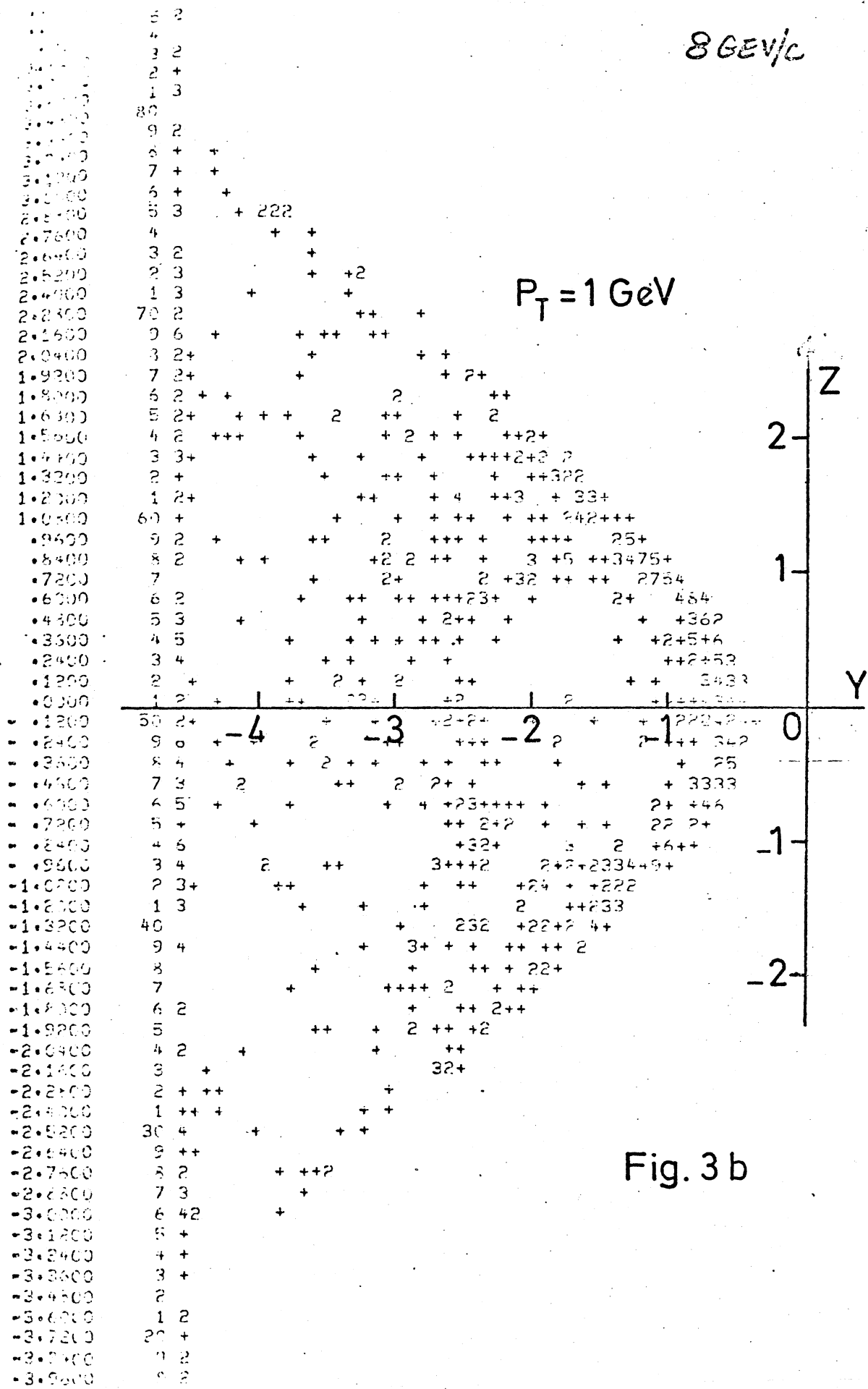
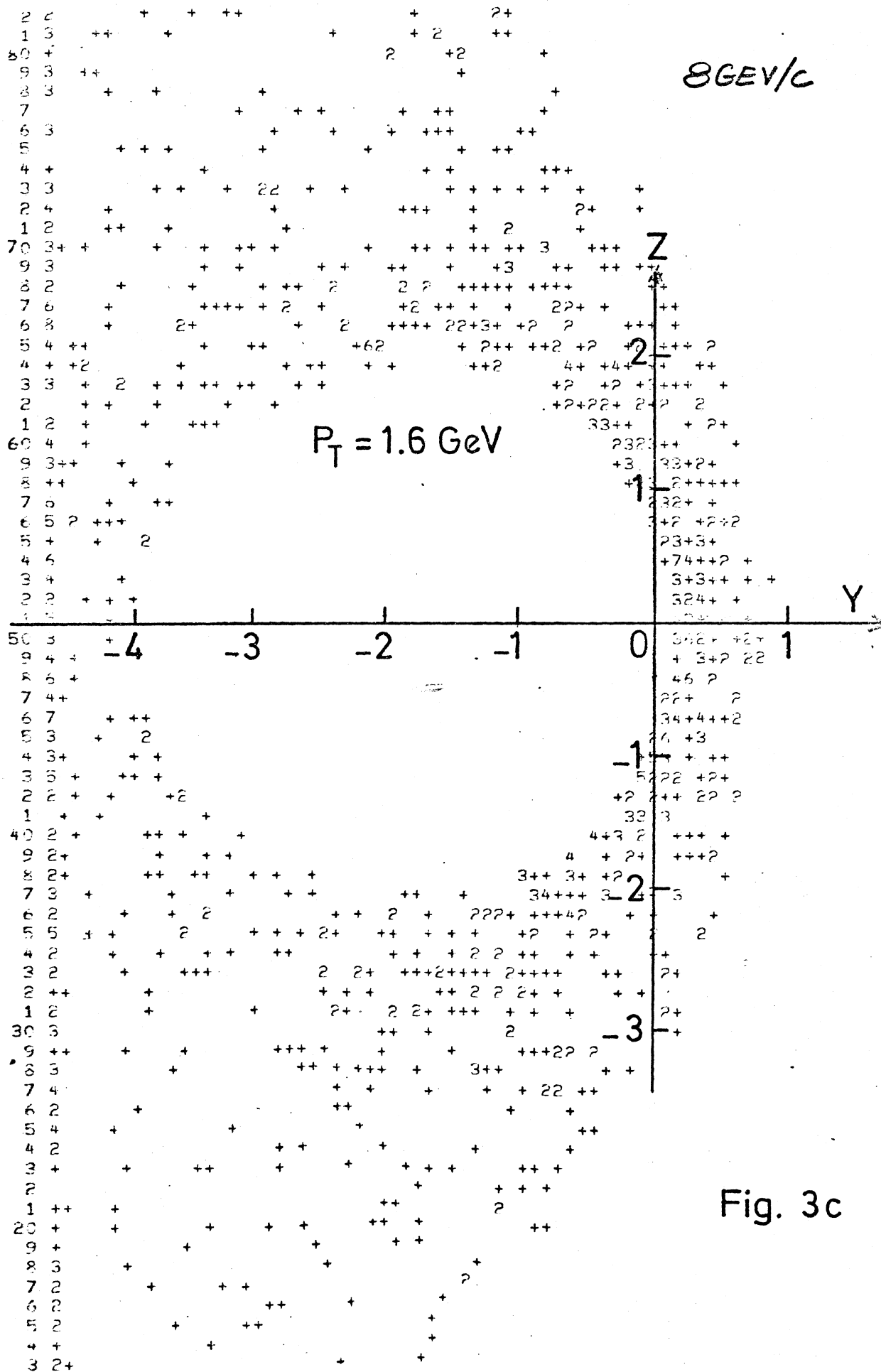


Fig. 3 b

2000  
 1800  
 1600  
 1400  
 1200  
 1000  
 800  
 600  
 400  
 200  
 0  
 -200  
 -400  
 -600  
 -800  
 -1000  
 -1200  
 -1400  
 -1600  
 -1800  
 -2000



8 GeV/c

$P_T = 1.6 \text{ GeV}$

Fig. 3c



8 GEV/C

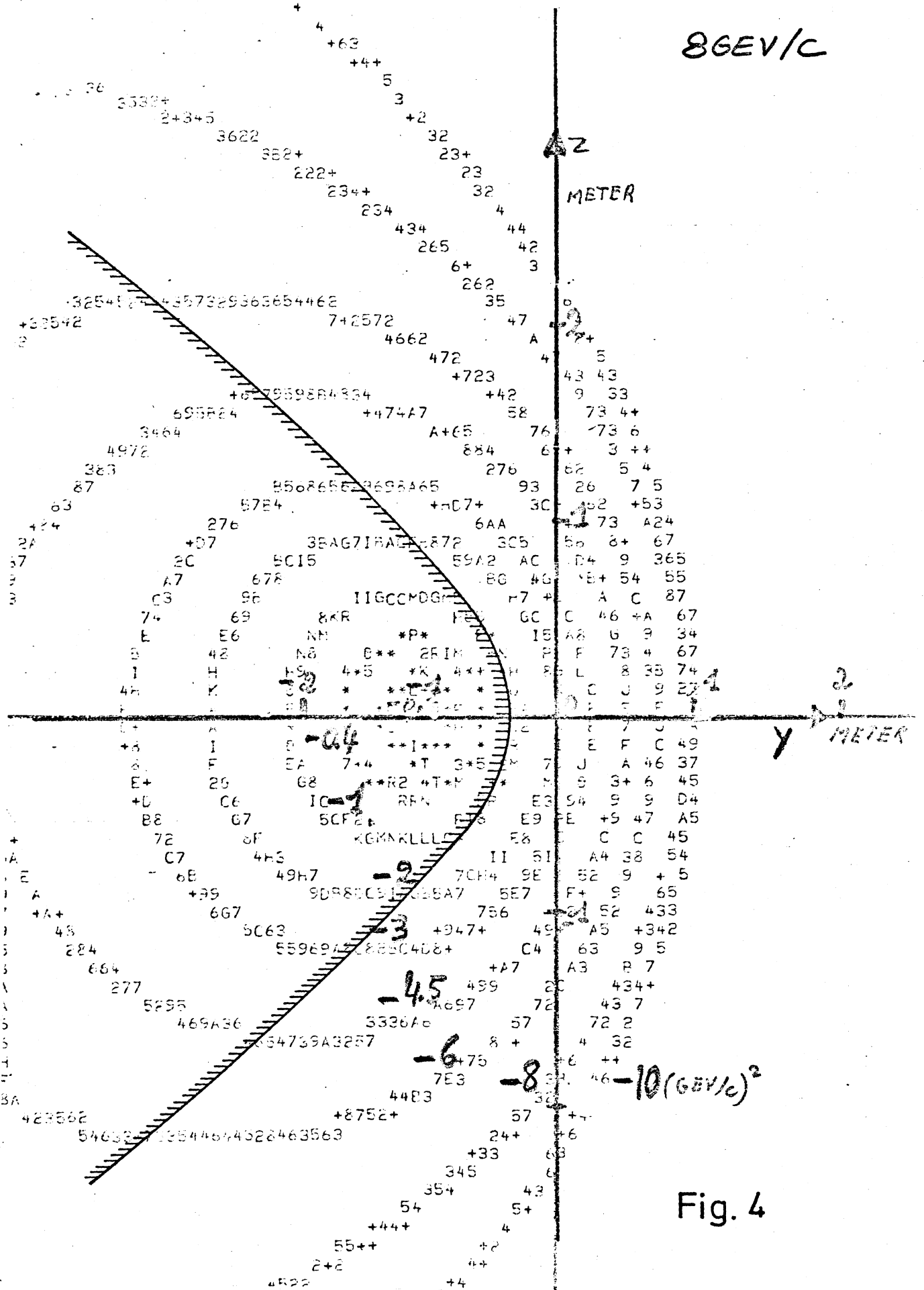


Fig. 4

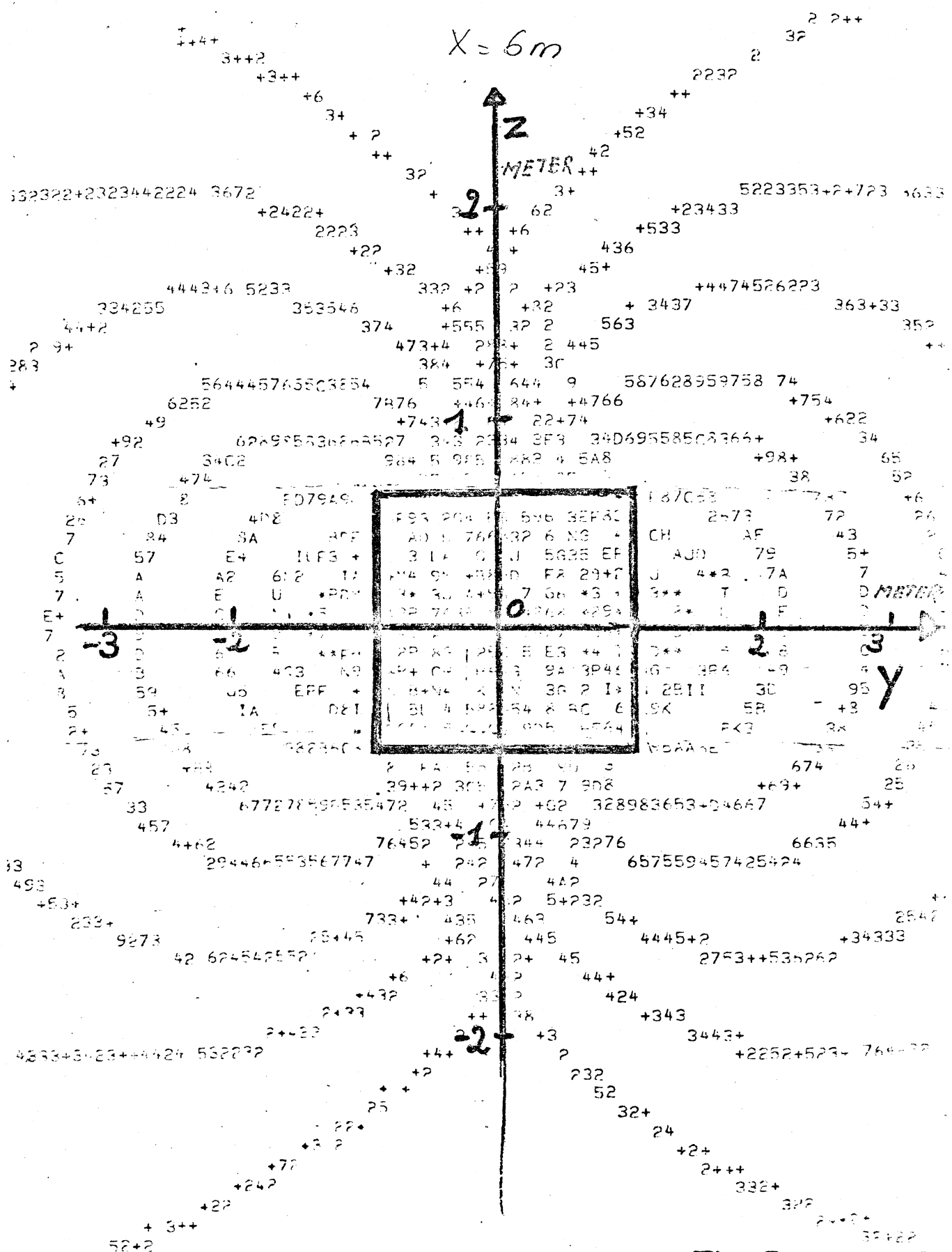


Fig. 5

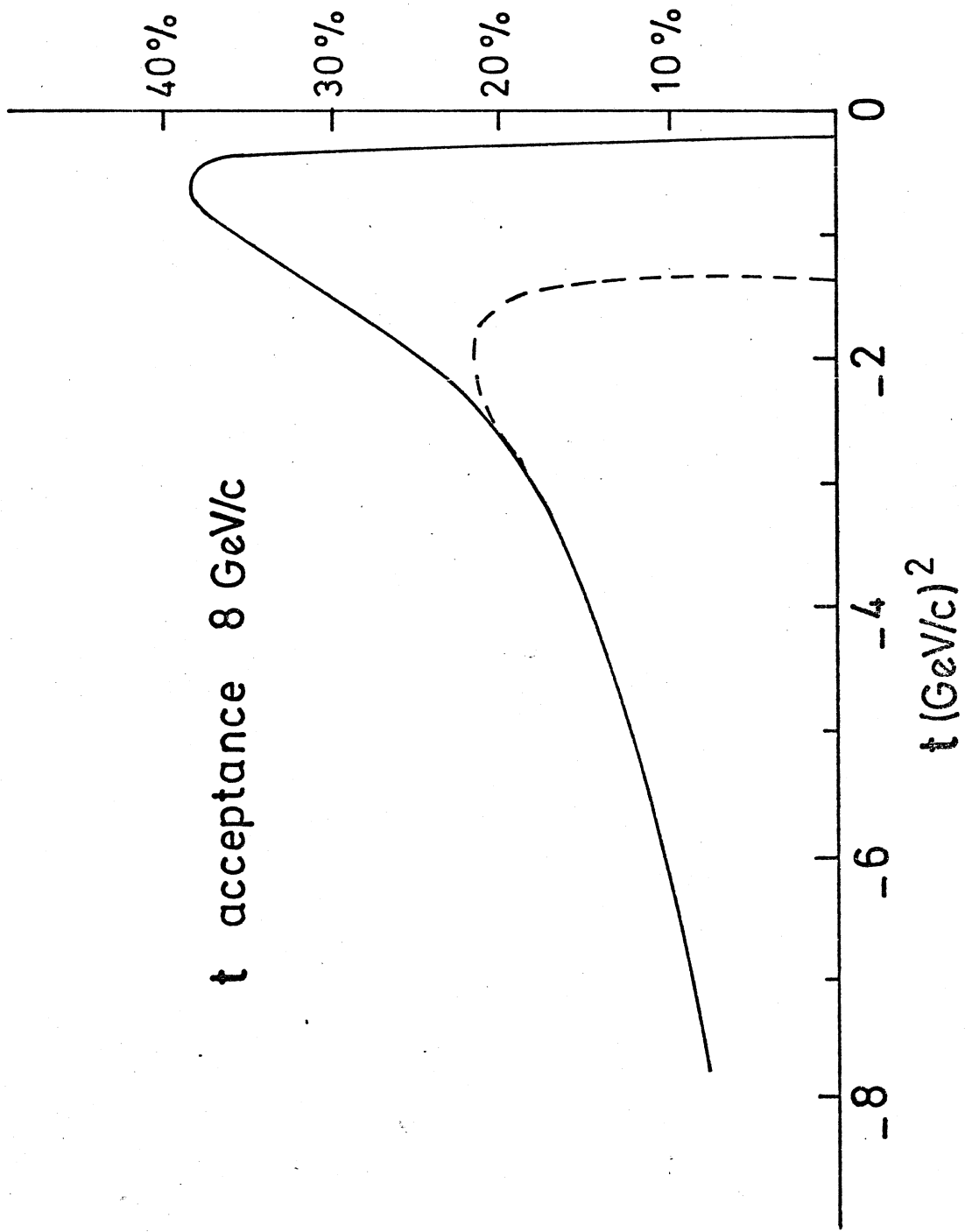


Fig. 6

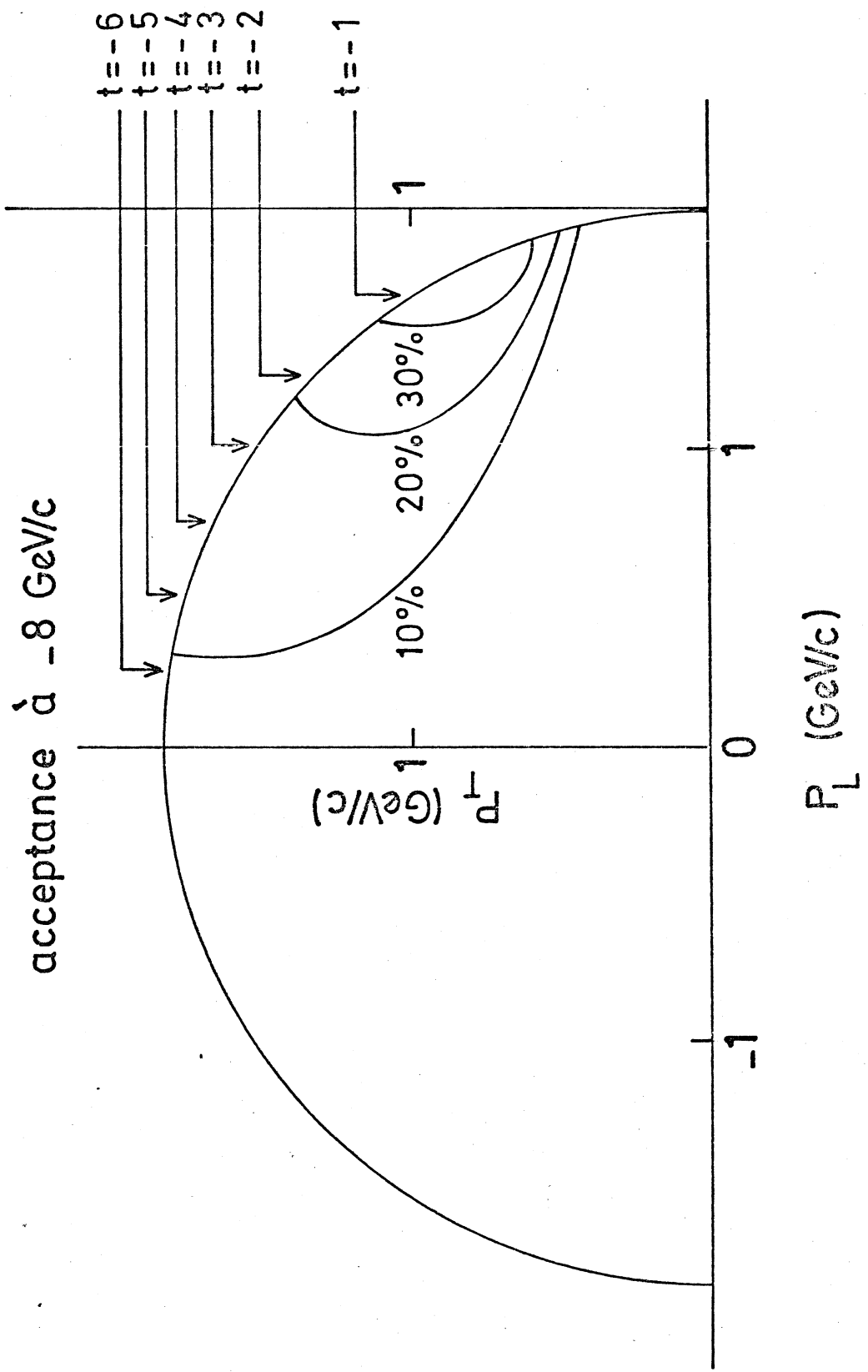


Fig. 7

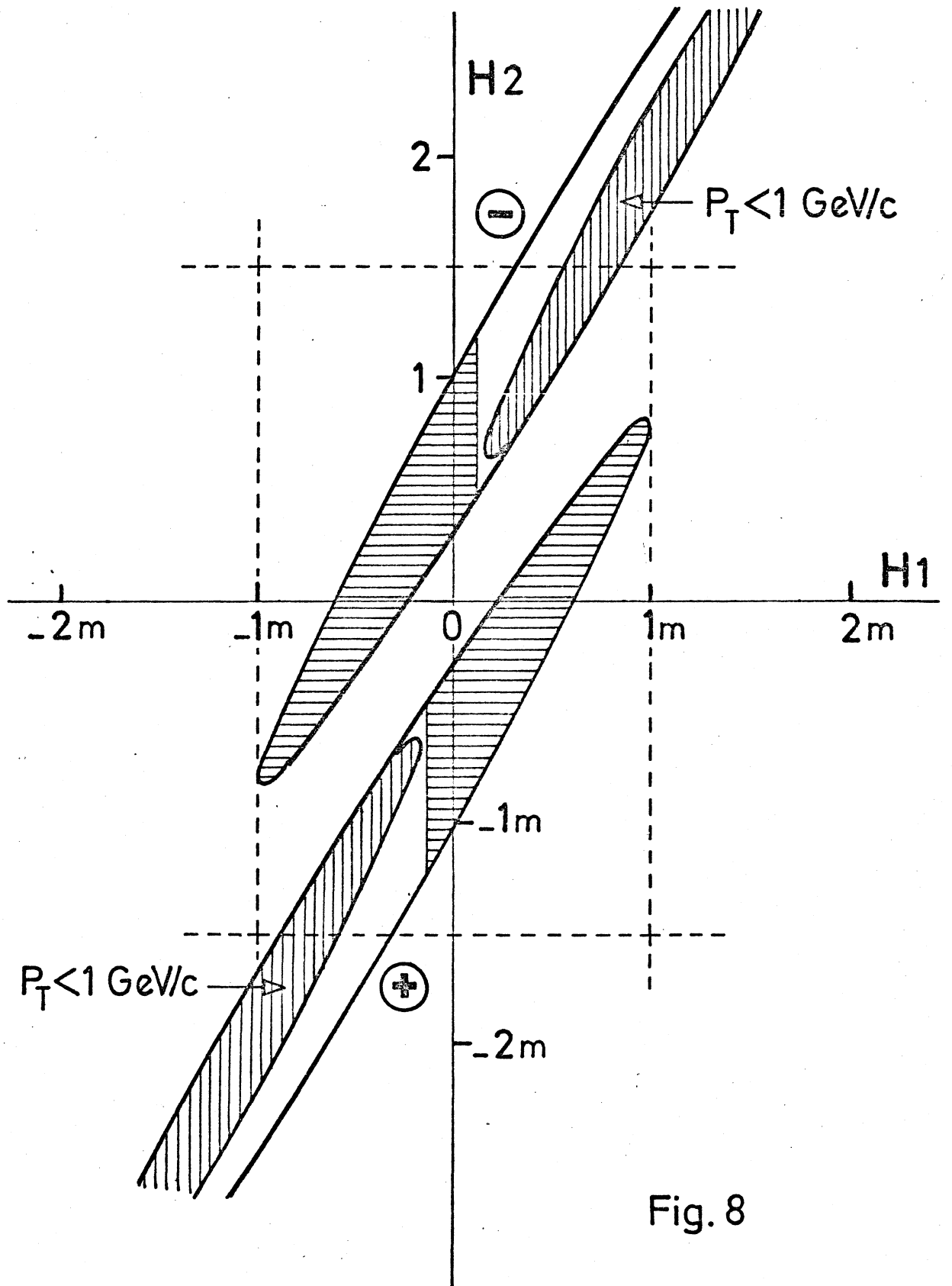


Fig. 8

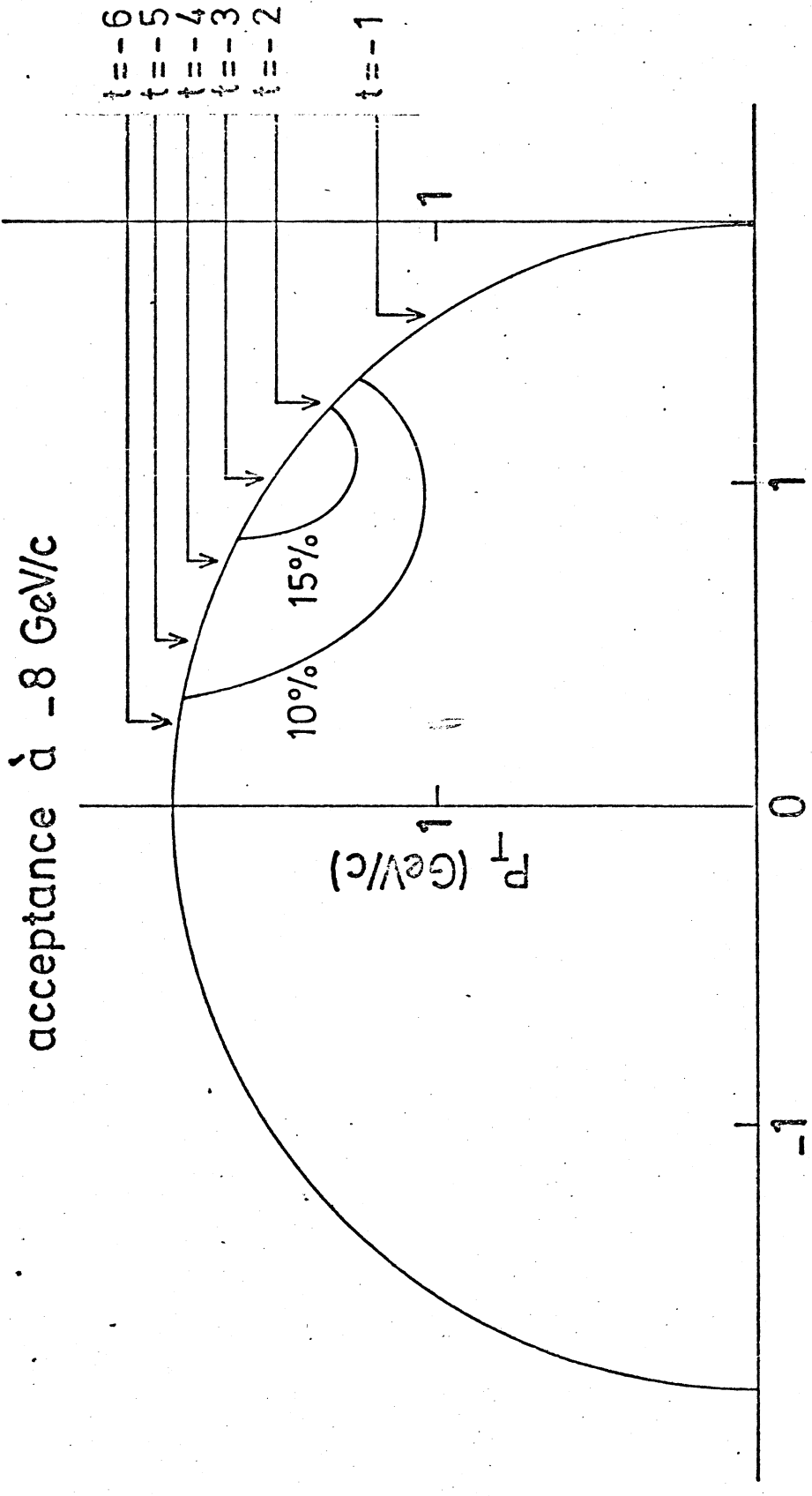


Fig. 9

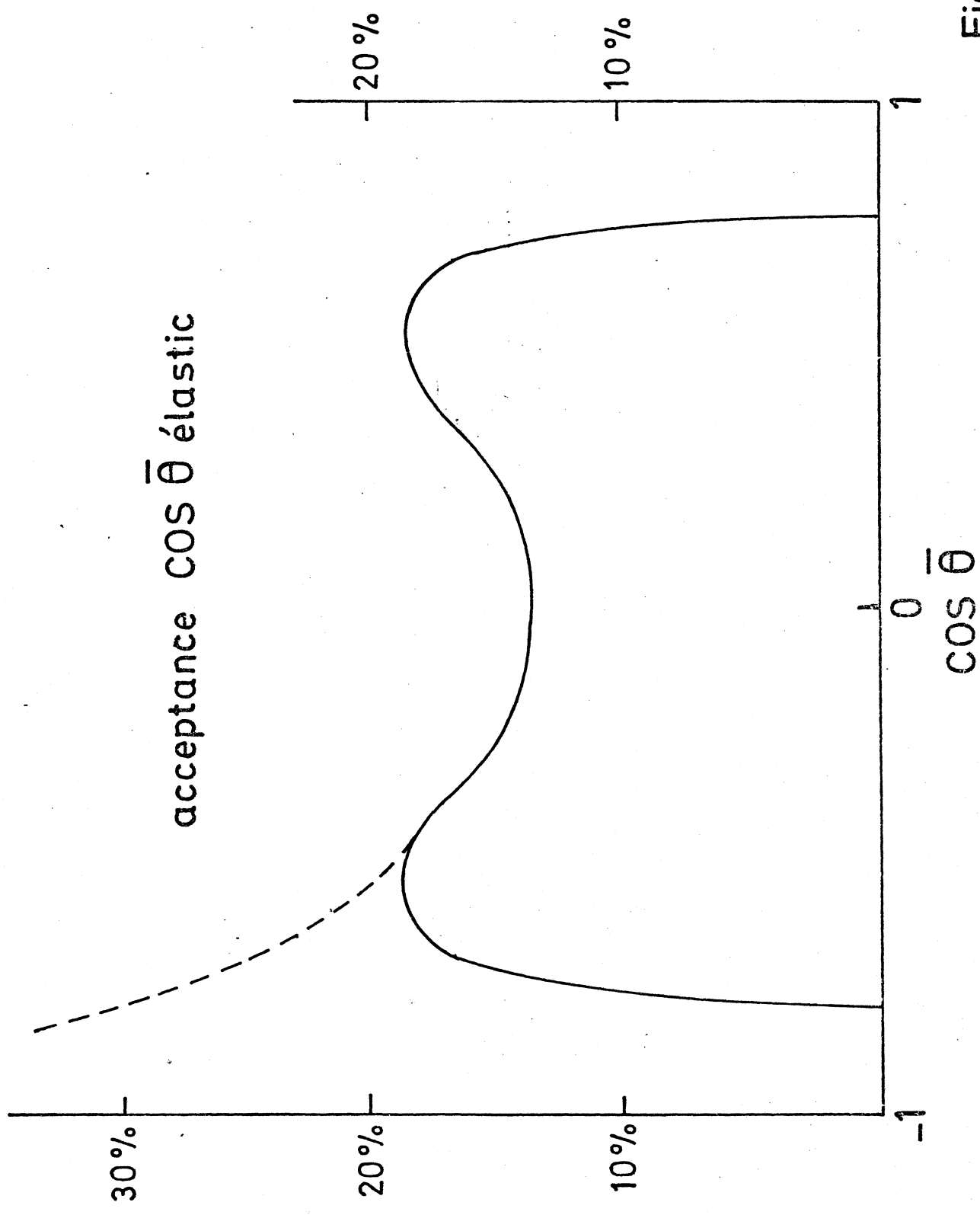


Fig.10